MIG-Assisted Kernel-Enabled Robot (MAKER) Arm for Seamless Automobile Maintenance and Service

Hwang-Cheng Wang[1,*], Sai Srinivas Vara Prasad Korlam[2], Manideep Reddy[2] and Harshith R Prasad[3]

[1]National Ilan University, No. 1, Section 1, Shennong Rd, Yilan City, 260007, Yilan County, Taiwan

[2]Vel Tech University, Avadi, Chennai, 600062, Tamil Nadu, India

[3]Presidency University, Itgalpur Rajanakunte, Yelahanka, Bangalore, 560064, Karnataka, India

Abstract: There is a definitive increase of excellence in the field of robotic automation, with automated vehicles that can drive people anywhere to automated robots that can perform high-risk surgeries remotely. Robotic automation was initiated as an industrial-grade asset capable of performing complex tasks and replacing humans limited by fatigue. With the advent and rise of Industry Revolution 4.0 (IR 4.0), in the modern world, one of the major markets that IR 4.0 occupies is the automobile industry. The automobile industry heavily employs robotic technology for vehicle manufacturing and assembly, yet post-sale servicing and maintenance remain predominantly manual. This discrepancy results in a gap in the efficient and timely maintenance of vehicles once they're in the hands of customers. According to a report of Allied Market Research [1], the expected Compound Annual Growth Rate (CAGR) of the global automobile repair and service market from 2022 - 2031 is expected at 7.6%, corresponding to 1,656.21 billion US dollars by 2031. This establishes the scale of the market that the proposed solution is going to be primarily based on. This paper proposes a MIG-based solution for providing welding service to damaged and sheared automobiles, thus reducing the stated discrepancy. The proposed solution creates a kernel environment where the twin-headed robotic arm can assess its surroundings and perform appropriate action from its operation pool using Reinforcement Learning and Machine Learning. The twin-headed robotic arm holds a torch and lead (Al) on the heads to perform the desired operations. This innovative approach is equipped with advanced sensors and programming to accurately detect, diagnose, and service vehicles by leveraging On Board Diagnostic (OBD) systems. This study delves into the theoretical and technical complexities of building an automated welder that explores the practical application of robotic technology in the automobile aftermarket. Notably, this technology promises improved accuracy, consistency, and timeliness in car maintenance, significantly reducing human error, improving service times, increasing productivity, and inducing economic growth.

Keywords: IR 4.0, Car service automation, Welding service, GMAW/MIG welding, OBD technology, Operation pool, Precision maintenance, IoT, AI.

1. INTRODUCTION

The automation industry, since its beginning to recent times, has been at the forefront of global economic harmony by continuously meeting the demand without burdening or increasing dependency on the human workforce. There are a few major stakeholders in the automation industry, of which the automobile/automobile industry is a significant confidant. The automobile industry, witnessing exponential growth along with the rapid expansion of the population, is undergoing a major transformation. In the pursuit of meeting escalating customer demands and augmenting production rates, automation robots have emerged as pivotal components in numerous industrial facilities [2]. This revolution in manufacturing is vital to strike a balance in the global supply chain and address burgeoning demands.

Since its beginning, the target of Industry Revolution 4.0, has been to induce Internet of Things (IoT) and servitization concepts into the global manufacturing industrial strategies [3]. All these strategies that are developed have different perspectives to address the design of manufacturing systems. Ultimately, they are dependent on two things: technology availability and its competent operation by workforce [4]. The contemporary scenario dictates that both production and service should be approached with utmost seriousness. Customers not only expect swift deliveries of products but also seek reliable aftercare services, which are instrumental not just for the proper functioning of the purchased products but also for maintaining a business's reputation. This, in turn, catalyzes increased sales due to the quality of aftercare provided to customers.

In the automobile realm, daily production rates have soared in response to the burgeoning population. Spectacles of cars being assembled in less than 30 seconds, where one caretaker oversees the production line while robotic automation orchestrates the process,

*Address correspondence to this author at the National Ilan University, No. 1, Section 1, Shennong Rd,, Yilan City, 260007, Yilan County, Taiwan;
E-mail: hcwang@niu.edu.tw

E-ISSN: 2409-9694/23

exemplify the industry's pace and reliance on advanced technology. However, a critical discrepancy emerges in the post-service phase: while a vehicle can be manufactured within a mere 30 seconds [5], the subsequent maintenance often takes considerably longer.

The issue at hand is evident-the majority of corporations in the automobile sector allocate insufficient emphasis on post-sale vehicle services. This oversight becomes increasingly conspicuous amid the rapid pace of manufacturing, reflecting a significant imbalance between production efficiency and the timely provision of maintenance services to consumers.

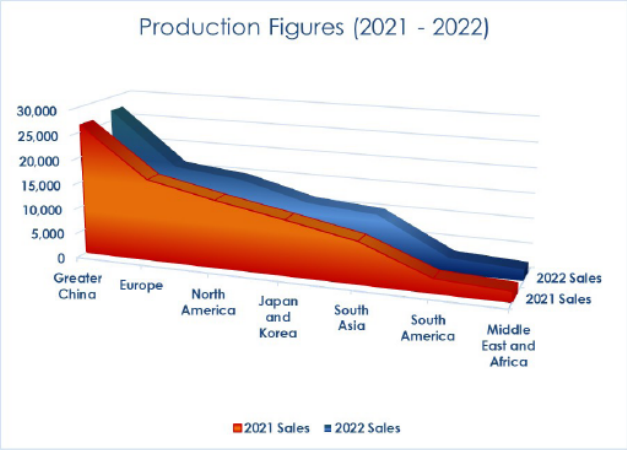

Figure 1: The projection of automobile sales (2021 - 2022) in various regions (based on the data at https://www.oica.net/category/production-statistics/2022-statistics).

Our research is poised to address this discrepancy by proposing the integration of sophisticated robotic systems, specifically focusing on the development and application of a specialized welding robot designed to streamline and enhance the maintenance process. There is an increase of 5.7% in automobile production between 2021 and 2022 as seen in Figure **1**. The statistics also reveal the annual repair of over 10 million cars through arc welding, with an average cost of $500 per repair [6], emphasizing the urgent need for a more efficient and advanced approach to automobile maintenance.

The foundation of our proposed solution lies in the utilization of robotic arms equipped with cutting-edge sensors and intricate programming designed to swiftly detect, diagnose, and execute precise maintenance tasks. Our endeavor is not just to identify faults but to promptly implement solutions [7]. The envisioned system primarily involves leveraging Gas Metal Arc Welding (Gas Metal Arc Welding (GMAW)/Metal Inert Gas (MIG)) to efficiently and accurately address the diverse maintenance needs of consumers.

This paper aims to meticulously explore the technical complexities involved in constructing these automated systems, emphasizing the practical application of robotic technology in the automobile aftermarket. The introduction of such advanced solutions promises not only increased accuracy, consistency, and timeliness in car maintenance but also a significant reduction in human errors, consequently reshaping the automobile experience for consumers [8].

Ultimately, this research aims to provide an accessible and affordable servicing of automobiles. By bridging the technological gap between manufacturing and post-sale vehicle maintenance, this proposal aims to enhance industry efficiency and elevate customer satisfaction, laying the groundwork for a new era in automobile maintenance.

2. METHODOLOGIES

2.1. Overview of the Proposed Solution

The research focuses on creating an indigenous, reliable solution for post-manufacturing service specifically designed to enhance the serviceability of damaged automobiles. This approach significantly contributes to the economic value chain by offering extensive repair services. The system is engineered to handle a variety of repair operations, such as welding cracks, reattaching sheared body parts, and employing suction pumps to fix dented areas. This comprehensive capability ensures that the system can effectively "heal" any shearing damage experienced by vehicles, improving their longevity and functionality.

To achieve this objective, the system is segmented into three primary components: the mechanical segment, the electronic segment, and the software processing segment. The mechanical segment is responsible for the physical repair tasks, utilizing specialized tools and mechanisms for precise welding and bodywork. The electronic segment includes the integration of ultrasonic sensors and other advanced technologies for detecting and analyzing damage. The software processing segment is dedicated to interpreting sensor data and guiding the repair processes, ensuring optimal accuracy and efficiency in every repair operation. This tripartite structure ensures a holistic and effective solution for automobile maintenance and repair.

2.2. Mechanical Segments of the Proposed System

The mechanical segment, particularly the development of a robotic arm for GMAW/MIG welding, is crucial in addressing the complex requirements of automobile repair. Similar research was conducted by Zamora-Nunez *et al*., where 304 stainless-steel plates were welded using a 45C8 medium carbon steel electrode in a GMAW process [9]. This study highlighted the importance of selecting ideal parameters for different configurations, especially considering the changes in the microstructure of the welded area [9]. GMAW/MIG welding is a very popular welding technique used in the automotive industry. It is a versatile and relatively easy-to-learn welding technique that can be used to weld a wide range of materials, including steel, aluminum, and stainless steel [10].

The mechanical segment of our GMAW/MIG welding robotic arm is a sophisticated integration of engineering tailored for automobile repair. It combines high-grade aluminum alloys for reduced inertia and steel in high-stress areas to withstand intense welding environments. The arm's design focuses on flexibility and reach, with an advanced system of joints and actuators enabling the welding torch to access tight spaces. Smooth movement of each joint is key to precise, steady torch handling, essential for quality welding. These metrics are determined by the degrees of freedom given to the mechatronic assembly. The degrees of freedom of the proposed solution can be assessed below.

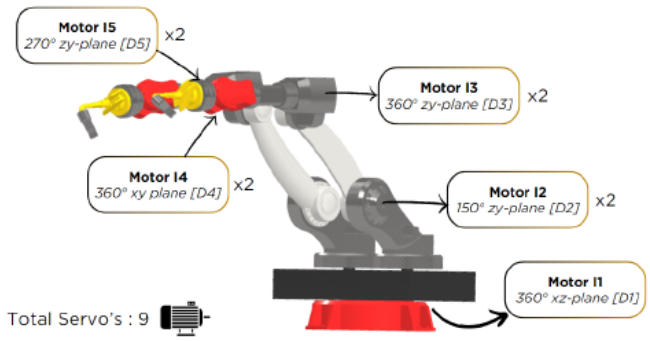

Figure 2: Placement of the servo motors in robotic arm.

Advanced servo motors provide fine control and responsive movement, vital for the precise tasks at hand. These motors are designed for durability and consistent performance, featuring high-duty cycles and built-in feedback systems. The process begins with the meticulous setup and calibration of the robotic arm, ensuring alignment with the designated welding path. The types of motors used in the MIG Assisted Kernel Enabled Robotic (MAKER) arm are motor 1 = 60 kg base, motor 2 = 50 kg, motor 3 = 30 kg, motor 4 = 20 kg, motor 5 = 15 kg, which makes a total number of 9 motors. The placement is depicted in Figure **2**

The system is then equipped with a wire electrode, the core material for the weld, and connected to a supply of shielding gas, typically a blend of argon and carbon dioxide, to protect the weld area from atmospheric contamination. Furthermore, the core parameters of GMAW, such as wire feed speed, welding voltage, welding speed, and the distance between the contact tube and workpiece, are pre-set and pre-programmed, with the capability for real-time adjustment. This flexibility is crucial as it allows for adaptive control over the welding current, which is a key factor in determining the arc power and, ultimately, the quality and consistency of the weld [11].

2.3. Electronic Segment

The mechanical segment constitutes the body to actuate the action, but the actuator and actuation are determined by the electronic segment. The electronic segment determines the need and application of multiple sensors, along with microcontrollers, to allow the smooth operation of the solution. This segment focuses on the electronic components that control and direct the mechanical actions of the system. Research in this field has demonstrated the reliability of automating welding processes using robotics. For instance, a GMAW operation was automated using the 'Fanuc Robot Arc Mate 100iC/12' robot, proving the feasibility and efficiency of such systems in real-world applications [12].

The primary operational circuit consists of Arduino Mega as the microcontroller, 11 motors with varying weight capacity, MPU6050, and Proportional – Integral – Derivative (PID) controllers. The accurate network of interactions can be seen in Figure **3**

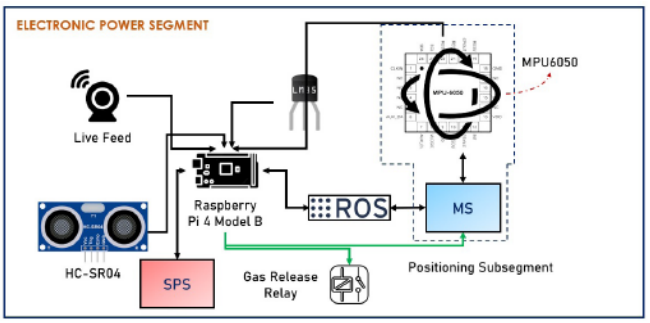

Figure 3: Architecture diagram of the electronic segment.

HARDWARE DESCRIPTION

1. Raspberry Pi 4 Model B: The Raspberry Pi 4 Model B is a powerful single-board computer that can be used as the main controller for the PID system. It has a quad-core ARM Cortex-A72 processor, 2GB of RAM, and a variety of connectivity options, including USB, Ethernet, and HDMI.

2. MPU6050: The MPU6050 is a 6-axis accelerometer and gyroscope that can be used to measure the orientation and motion of the Raspberry Pi. This information can then be used by the PID controller to adjust the motors and keep the Raspberry Pi stable.

3. Motors: The motors are used to move the Raspberry Pi in the desired direction. The specific type of motors that are used will depend on the application and position of the motor based on the requirement of the different loads and torque.

4. HDCAM: The HD camera is used to capture video footage of the Raspberry Pi's surroundings. This footage can then be used to help the PID controller track the Raspberry Pi's position and orientation. The module that is used in the arm is Camera Module V3. The Camera Module V3, released in 2023, has a 12-megapixel sensor and can capture still images and 4K video at 30 frames per second. It also has a wider field of view than the Camera Module V2.

2.4. Software Processing Segment

Software processing involves the development and implementation of algorithms for real-time decision-making and control. In line with this, a study on an automatic welding robotic arm system based on image de-noising explored the optimization of vision modules in robotic systems for improved accuracy and efficiency in complex environments [13]. There are two sub-modules in this particular segment; one is to detect cracks within the provided video media, and the other is the Reinforcement Learning (RL) agent, as depicted in Figure **4**.

The crack detection subsegment acts as the supportive component to the ultrasonic sensor to let Raspberry Pi know that it is in the right region. In simple words, the ultrasonic sensor is to find out the small-scale cracks, while the crack-detection subsegment is for identifying the bigger ones [26].

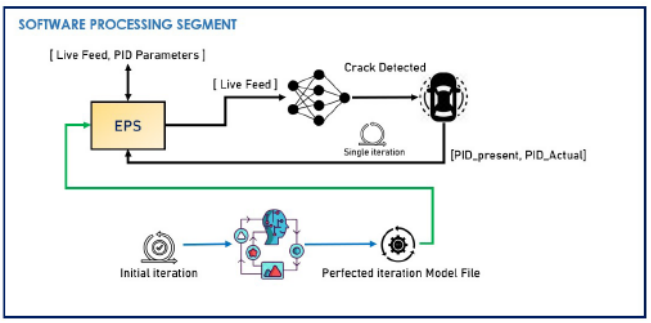

Figure 4: Architecture diagram of the software processing segment.

To identify such minute damages, the processing power of the neural network should not only be high but also ideal. The neural network should be able to give fast and accurate outputs with minimum load. As compared to other models, Deep & Cross Network (Deep Cross Network (DCN)) holds the best and deepest impact over car damage assessment [14]. Backed by the data plot in Figure **5**, it can be determined that DCN gives one of the most accurate outputs for crack damage. Note that ResNet-50 and ResNet-101 are backbones used as support for different models such as DCN, Mask Region-based Convolutional Neural Network (RCNN), Faster RCNN, etc.

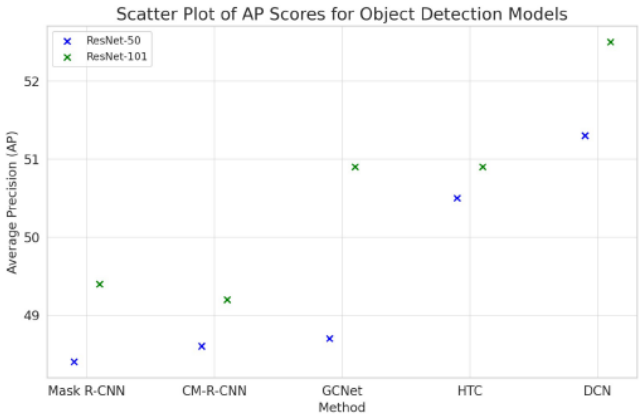

Figure 5: AP comparison of object detection models on ResNet-50 and ResNet-101 backbones.

Feedback is probably one of the most important and core principles of automation because learning is a gradual change from wrong choices to right choices. The RL Agent works similarly. It trains the model rigorously to perfection, thus entailing the output to be as close to perfect action as possible. There are two types of feedback loops in the proposed solution, namely, PID Library and Reinforcement Learning (RL) Agent. The RL agent is trained before deployment, using countless simulation outcomes utilizing the

reward and cost function. Once the result is acceptable, it is deployed within the machine. The optimal reward-cost trade-off implies the best possible decision that the RL agent can generate. This plot can be found in Figure **6**.

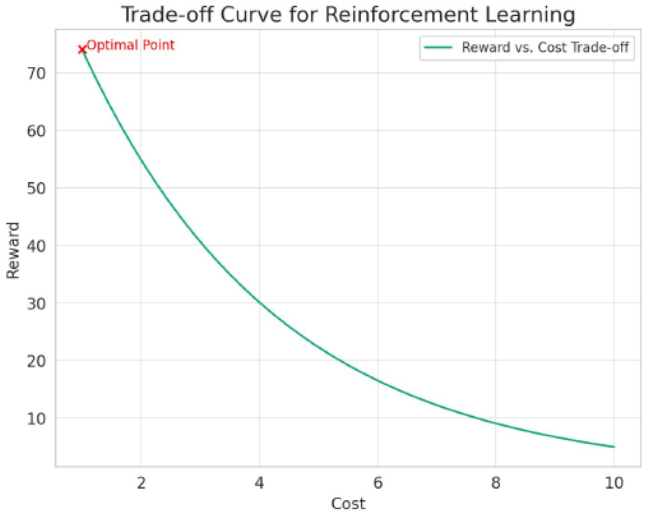

Figure 6: Trade-off curve between reward and cost for a reinforcement learning agent, highlighting the optimal balance point for deployment.

Here comes the use of Proportional-Integral-Derivative (PID), which would be connected to ROS, that directs all the changes and corrections necessary to achieve the target outcome and action. It is explained below:

1. Proportional Control (P): This part of the PID controller reacts to the current error, which is the difference between the desired set point and the current state. In the robotic arm, this would adjust movements proportionally to the error, helping the arm to reach the target position or state more accurately.

2. Integral Control (I): The integral component sums up past errors to determine the cumulative offset that the system has encountered over time. This is useful in eliminating any residual steady-state error by adding a control effect based on the historic cumulative error, thereby ensuring the robotic arm's precision over continuous operations.

3. Derivative Control (D): This aspect focuses on the rate of change of the error, providing a predictive control. It dampens the system's response to avoid overshooting the set point. In the robotic arm, this would mean anticipating future movements and adjusting the current motion to smooth out the trajectory.

3. PROCESS FLOW AND METHOD PARTICULARS

The automation process of the proposed solution has various parts and sub-operations that bring about a required action. At each and every step of the way, there is a stark need to understand the data flow and operation execution. In order to understand this further, the flow chart diagram in Figure **7** is clearly depicted.

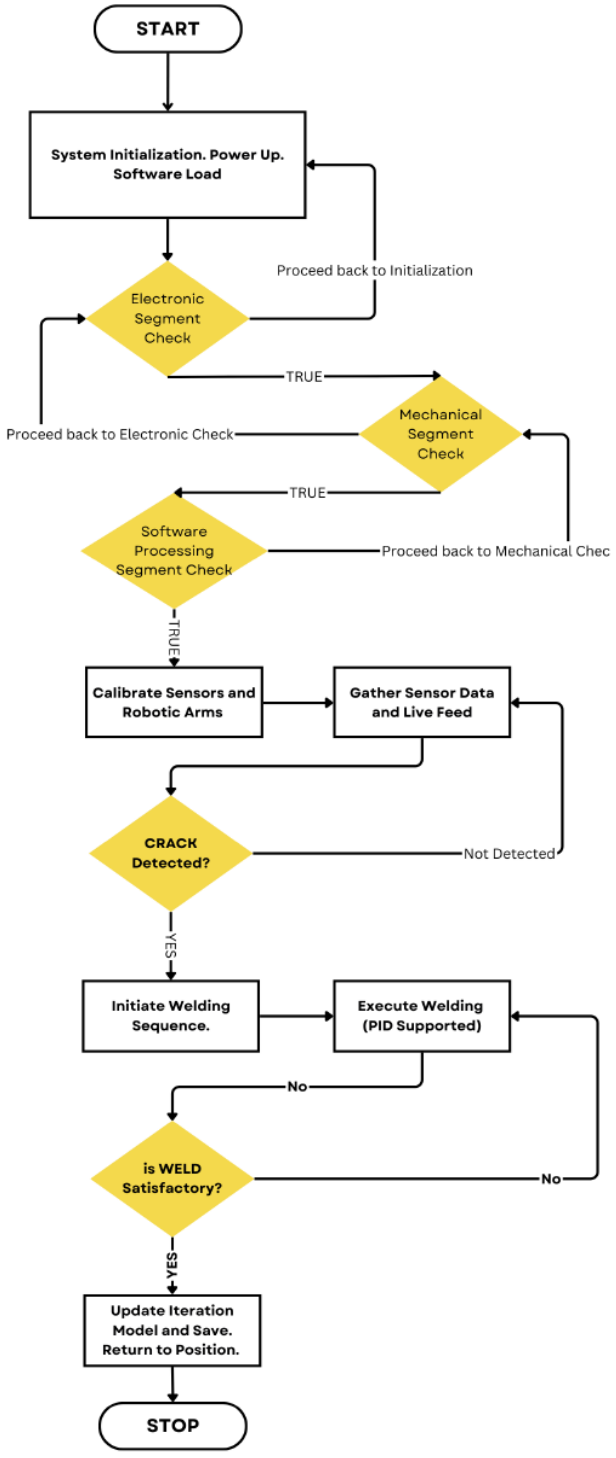

Figure 7: Process flow of the whole system.

The mobility and reach of the final arm can be determined by the degrees of freedom of the mechatronic assembly. For the set assembly, there are five degrees of freedom, denoted by D_i, where $i \in [1,5]$. The different degrees of freedom for the given assembly can be found in Figure **8**. Every degree of freedom has an assigned action, which is precisely discussed below:

1. Base Rotation (1st Degree of Freedom) D_1:

(a) This allows the robotic arm to swivel around a vertical axis.

(b) Crucial for aligning the arm with the workpiece from various angles.

2. Shoulder Movement (2nd Degree of Freedom) D_2:

(a) Similar to a human shoulder, it enables the arm to move forward and backward.

(b) Essential for adjusting the arm's reach and accessing different points on a large workpiece.

3. Elbow Movement (3rd Degree of Freedom) D_3:

(a) Functions like a human elbow, bending to extend or retract the arm's lower segment.

(b) Allows for fine-tuning the arm's position, especially in complex welding tasks.

4. Wrist Pitch (4th Degree of Freedom) D_4:

(a) Enables the wrist of the robotic arm to tilt up and down.

(b) Key for precision welding tasks, ensuring the torch maintains the correct angle relative to the workpiece.

5. Wrist Roll (5th Degree of Freedom) D_5:

(a) Allows the wrist to rotate the welding torch.

(b) Vital for tasks that require welding at various angles or in circular patterns.

Subsequently, defining the clear and crypt requirement of movement space for each sub-part of the assembly is crucial. The base joint (D_1) allows for full 360° rotation in the horizontal plane, offering the arm a comprehensive swivel range at its foundation. The shoulder joint (D_2) articulates in a 150° arc within the vertical plane, providing elevation and depression from the horizontal baseline. The elbow joint (D_3) extends the arm's reach, with a 360° rotation capability around the arm's longitudinal axis. The wrist motion (D_4) has a 270° movement range, which grants the end effector the ability to tilt and orient the welding torch extensively. Finally, the torch motion (D_5) is capable of full 360° rotation in the xy-plane, which ensures that the torch can be accurately positioned for welding at any required angle [15].

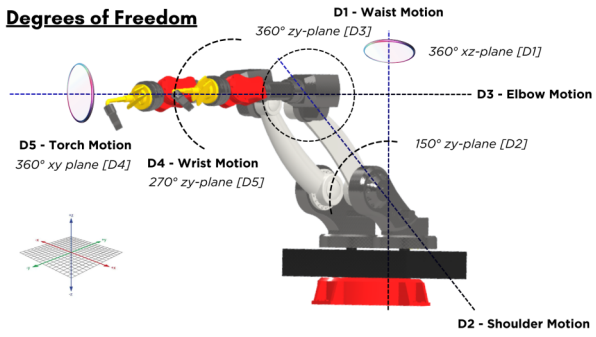

Figure 8: Robotic arm with 5 DOF (degrees of freedom).

3.1. Kinematic Chain and Transformation Matrices

Any mechatronic assembly is backed up with a relevant kinematic design that drives the body forward. The MAKER's kinematic design begins with the placement and positioning of the collective joints and links, which correspond to real-world actuators and body parts. This collective is called the kinematic chain. A kinematic chain is defined as a series of linkages that join the joints and links together to form a common body that has individual inertial motions [16]. The kinematic chain formed by the mechatronic assembly can be seen in Figure **9**.

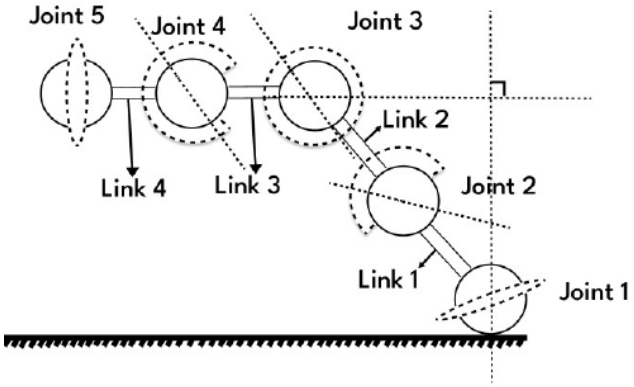

Figure 9: Kinematic chain of the mechatronic assembly.

Furthermore, the next basic terminology that drives the assembly is dependent on transformation matrices, which determine the different states that the robotic arm goes through in order to meet the requirements. A transformation matrix is a mathematical construct that describes the position and orientation of one link of the robotic arm relative to another link or the base frame. Specifically, for a robotic arm with joints and links, the transformation matrix encapsulates the spatial relationship between consecutive joints or between the base and the end-effector (welding torch).

Each transformation matrix is typically a 4x4 matrix in homogeneous coordinates, which includes both linear transformations (for position) and rotational transformations (for orientation), as well as a row for perspective transformations (which, in the case of robotic arms, is usually [0 0 0 1] since there are no perspective transformations involved).

Here is what the structure of a transformation matrix looks like

$$\begin{bmatrix} (R_{11}) & (R_{12}) & (R_{13}) & (P_x) \\ (R_{21}) & (R_{22}) & (R_{23}) & (P_y) \\ (R_{31}) & (R_{32}) & (R_{33}) & (P_z) \\ 0 & 0 & 0 & 1 \end{bmatrix} \quad (1)$$

where

• The upper left 3x3 submatrix (R) consists of the rotation matrix, which represents the orientation of the end-effector relative to the base frame.

• P_x, P_y, and P_z are the components of the position vector, representing the position of the end of one link relative to the other in the base frame coordinates.

• The last row is for homogeneous coordinates, which makes it possible to perform linear transformations and translations in a single matrix multiplication.

For each joint i in the arm, we can define a transformation matrix ${}^{i-1}T_i$ that transforms the coordinates from the frame of joint $i-1$ to the frame of joint i. By multiplying these matrices together sequentially, we can calculate the overall transformation ${}^{0}T_n$ from the base of the robotic arm to the end-effector. This allows us to determine the exact position and orientation of the welding torch based on the angles of the joints, which is critical for the precise control needed in welding applications.

Therefore, we have a total of 5 joints and 4 revolute links. Thus, forming the transformation matrices of each joint gives us the final position and orientation of the mechatronic assembly. To evaluate these matrices, the Denavit-Hartenberg (D-H) convention is used. This method standardizes the frame assignment process and simplifies the computation of transformation matrices. Here is how to construct the D-H parameters and transformation matrices for each link:

1. D-H Parameters Assignment: for each joint i, the D-H parameters to be defined are:

(a) θ_i: The joint angle between the previous x-axis and the current x-axis, measured about the previous z-axis.

(b) d_i: The offset along the previous z-axis to the common normal.

(c) a_i: The length of the common normal (distance between the z-axes of two consecutive links, *i.e.*, link length).

(d) α_i: The angle between the previous z-axis and the current z-axis, measured about the common normal (current x-axis).

As Link 1 remains stationary and all joints operate as revolute joints, Link 1 serves as the fixed offset for the initial joint, while the subsequent links vary at each joint, contributing to the dynamic flexibility design.

2. Individual Transformation Matrices: Each transformation matrix $\left({}^{i-1}A_i\right)$ from frame $i-1$ to frame i for $i \in [1,5]$ is defined as:

$${}^{i-1}A_i = \begin{bmatrix} \cos\theta_i & -\sin\theta_i\cos\alpha_i & \sin\theta_i\sin\alpha_i & a_i\cos\theta_i \\ \sin\theta_i & \cos\theta_i\cos\alpha_i & -\cos\theta_i\sin\alpha_i & a_i\sin\theta_i \\ 0 & \sin\alpha_i & \cos\alpha_i & d_i \\ 0 & 0 & 0 & 1 \end{bmatrix}$$

3. Overall Transformation Matrix: Multiply the individual transformation matrices to get the overall transformation matrix from the base to the end-effector, as shown in equation (2):

$${}^{0}T_5 = {}^{0}A_1 \cdot {}^{1}A_2 \cdot {}^{2}A_3 \cdot {}^{3}A_4 \cdot {}^{4}A_5 \quad (2)$$

This matrix represents the pose of the end-effector in the base frame.

3.2. Forward and Inverse Kinematics

The forward kinematics of a mechatronic chain assembly is instrumental in defining the positional and orientational relationship between two consecutive links, given known link parameters and angular positions. This kinematic analysis primarily serves to determine the precise location and orientation of the end-effector about the base link, a crucial aspect for effective operational control [17]. Forward kinematics (FK) in robotics involves calculating a robot's center of mass for balance and stability, crucial for safe and efficient operation. This process follows a unidirectional flow from the robot's base to its end-effector. Specifically, for a robotic arm, FK entails the sequential multiplication of transformation matrices corresponding to each joint's movement, progressing from the base to the end-effector. This produces a final transformation matrix that defines the end-effector's position and orientation in the workspace. FK is deterministic; a specific set of joint angles yields a unique end-effector pose. The final transformation matrix in equation (2) represents the end-effector's base position in the workspace.

1. Extract the Position Vectors:

- The position (x, y, z) of the end-effector is given by the elements P_x, P_y, P_z, of the transformation matrix.
- $$Position = \begin{bmatrix} P_x \\ P_y \\ P_z \end{bmatrix}$$

2. Determine the Orientation of the End-Effector:

- The orientation can be described using different conventions, such as Euler angles, axis-angle, or quaternions. For simplicity, we'll use Euler angles (roll, pitch, yaw).
- The Euler angles can be calculated from the rotation matrix. Assuming a ZYX rotation sequence, we have:

  - Roll $(\varphi): arctan(2(R_{32}, R_{33}))$

  - Pitch $(\theta): arctan(2(-R_{31}, \sqrt{R_{32}^2, R_{33}^2}))$

  - Yaw $(\psi): arctan(2(R_{21}, R_{11}))$

- $$Orientation = \begin{bmatrix} \phi \\ \theta \\ \psi \end{bmatrix}$$

3. Combining Position and Orientation for Target Pose:

The target pose of the end-effector is a combination of its position and orientation:

$$Pose = \begin{bmatrix} Position \\ Orientation \end{bmatrix}$$

Inverse kinematics, the counterpart to forward kinematics, determines joint angles based on a desired link position and orientation. This calculation is essential for directing a robot's end-effector to a specific point in space using known geometric link parameters. Unlike forward kinematics, it often presents multiple or no solutions, adding complexity to robotic path planning and control.

3.3. Motion Dynamics

When conducting motion dynamics analysis for a robotic arm, the process is rooted in classical mechanics, particularly the study of forces and motion of rigid bodies. While the kinetic analysis of mechatronic assembly holds energy responsible for motion, the kinematic / motion dynamics is essential to recognize the forces acting upon the assembly [27]. The study is divided into two main areas: forward dynamics and inverse dynamics.

Forward dynamics, also known as direct dynamics, focuses on determining the accelerations and subsequent motion of the robot's links given a set of forces and torques. This aspect is crucial for simulating the robotic arm's behavior under various conditions and is typically employed in the design and testing phases. The governing equation for forward dynamics is derived from Newton's second law of motion and can be expressed in the form of equations that relate forces to the accelerations they produce:

$$\boldsymbol{F} = m\boldsymbol{a} \tag{3}$$

where $\boldsymbol{F}$ represents the force vector, m is the mass of the object, and $\boldsymbol{a}$ is the acceleration vector.

Inverse dynamics, on the other hand, deals with the calculation of forces required to produce a desired acceleration. This process is fundamental for the control of robotic arms, especially in tasks that require precise movements, such as assembly operations, painting, or surgery. By computing the necessary torques at the joints, engineers can create control algorithms that ensure the robotic arm moves along a predetermined path with the desired speed and precision.

The mathematical foundation of robotic arm motion dynamics is encapsulated in the equations of motion. The kinetic energy of the system is often represented in quadratic form, reflecting the interplay between mass distribution and velocity. The equation for kinetic energy K is given by:

$$K = \frac{1}{2}\boldsymbol{q}^T \boldsymbol{M}\boldsymbol{q} \tag{4}$$

where $\boldsymbol{q}$ is the vector of generalized coordinates, and $\boldsymbol{M}$ is the mass matrix of the robotic arm.

Inertial forces play a crucial role in the dynamics of a robotic arm. The moment of inertia, which quantifies a body's resistance to changes in rotational motion, depends on the mass distribution relative to the axis of rotation. The inertial force for each link of the robotic arm can be expressed as:

$$I = \sum_{i=1}^{n} m_i r_i^2 \tag{5}$$

where the moment of inertia *(I)* for a rotating body is defined as the sum of the products of the mass (m) and the square of the distance *(r)* from the axis of rotation for all its constituent parts.

To encapsulate the dynamic behavior of the robotic arm, the Newton-Euler formulation is employed. This set of equations combines Newton's laws for translational motion and Euler's laws for rotational motion, resulting in a comprehensive model that accounts for both linear and angular velocities, as well as the forces and torques acting on the robot's joints. The overall dynamics of the robotic arm in joint space can be summarized by the equation:

$$\boldsymbol{M}(\boldsymbol{q})\ddot{\boldsymbol{q}} + \boldsymbol{V}(\boldsymbol{q},\dot{\boldsymbol{q}}) + \boldsymbol{G}(\boldsymbol{q}) = T(\boldsymbol{q}) \tag{6}$$

Here, $\boldsymbol{M}(\boldsymbol{q})$ represents the mass matrix, $\ddot{\boldsymbol{q}}$ denotes the second derivative of the vector $\boldsymbol{q}$, and $\dot{\boldsymbol{q}}$ represents the first derivative of $\boldsymbol{q}$. $\boldsymbol{V}(\boldsymbol{q},\dot{\boldsymbol{q}})$ denotes the Coriolis and centrifugal forces calculated over time, $\boldsymbol{G}(\boldsymbol{q})$ is the gravity force vector, and $T(\boldsymbol{q})$ denotes the generalized forces acting on the system.

3.4. Machine Learning Model Detail

As discussed earlier, there are two base learning models that act as the core processing programs for driving the choice and decision of the machine. The first model is the *crack detection model*, a specialized convolutional neural network designed to process visual data from cameras attached to the robotic arm. This model has been trained on a vast dataset of images annotated with various types of crack damage, enabling it to distinguish between significant cracks and negligible anomalies with high precision.

The core intelligence of the automatic welding robotic arm system is driven by two principal learning models. The crack detection model harnesses a convolutional neural network to process visual data and discern substantial crack damages from minor surface imperfections, enhancing the precision of the arm's operations. On the other side, the *reinforcement learning (RL) Agent* diverges from conventional control systems by employing trial-and-error methods to optimize action strategies, hence improving the arm's performance over time.

The amalgamation of these models within a high-caliber computational framework ensures swift and accurate responses essential for real-time tasks [18]. This collaborative operation of the models facilitates not just immediate corrections but also prescient adjustments, propelling the system well beyond the capabilities of traditional automated solutions. Advanced algorithms within the PID controller finely tune each of its components-Proportional, Integral, and Derivative-tailoring them to the arm's dynamics, which affords an unparalleled level of operational finesse, ensuring the robotic arm meets both current and future demands with unwavering precision.

4. RESULTS AND DISCUSSION

4.1. Robotic Arm Functionalities

The robotic arm developed for our project represents a significant advancement in the field of industrial automation, particularly in the context of Gas Metal Arc Welding/Metal Inert Gas for automobile maintenance. This robotic arm is not just a piece of machinery; it's an intricate system designed to enhance precision, efficiency, and safety in welding tasks. At its core, the arm's functionality revolves around performing detailed and high-quality welding operations, crucial for repairing and maintaining various automobile parts. Its design caters specifically to the unique challenges posed by automotive repair [19], which often involves working in tight spaces and on complex geometries that demand a high degree of precision and adaptability.

This robotic arm is unique due to its specialized design for Gas Metal Arc Welding (GMAW) or Metal Inert Gas (MIG) welding processes, a method widely

recognized for its efficiency and effectiveness in automotive applications. The arm is equipped with advanced features such as ultrasonic sensing, which allows for real-time detection of discrepancies in metal joints, ensuring that welding is performed with maximum accuracy. Additionally, the dual-arm structure of the system enhances its functionality significantly. One arm is dedicated to manipulating the welding torch with remarkable precision, while the other assists in adjusting the welding head for optimal access to welding points or positioning the workpiece [20]. This coordinated movement between the two arms is critical for complex welding tasks, enabling the system to handle a wide range of welding operations with enhanced control and stability.

4.2. Kinematic Analysis

Degrees of Freedom and Range of Motion: The robotic arm features five distinct degrees of freedom, which enable it to maneuver and orient the welding torch with high precision. The interplay of these movements ensures the welding torch can be manipulated precisely, maintaining optimal angles and distances from the workpiece [25], which is crucial for achieving high-quality welds. As shown in Figure **10**, the torque for individual joints has been computed and calculated accordingly, thus allowing the evaluation of the final inertial torque.

Kinematic Chain and Transformation Matrices: In the kinematic chain of this arm, each joint's movement is interconnected, with the position and orientation of each link impacting the subsequent one. The kinematic chain is typically defined using transformation matrices that express the relationship between the joints. For each joint, a transformation matrix is constructed [13] that describes the position and orientation of that joint relative to the previous one, ultimately leading to a cumulative transformation matrix that describes the position and orientation of the torch in space.

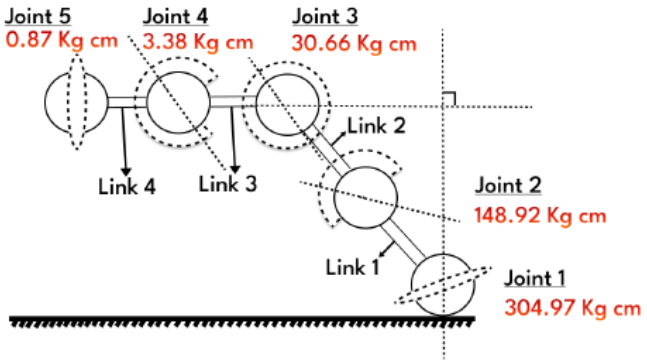

Figure 10: Individual torque values at each DOF.

As detailed in Table **1**, the lengths vary considerably, with the shortest link being 6.12 cm and the longest extending to 31.73 cm. These variations allow the arm to execute complex movements with precision, essential for tasks requiring high dexterity and spatial accuracy. Each link's length contributes to the overall kinematic chain, determining the arm's reach and capability to maneuver in confined spaces. This reach is substantiated by the individual torque force applied on its respective joints.

The histogram graph presents the distribution of joint distances for a robotic arm in Figure **11**, based on a simulated dataset. It illustrates the frequency at which the arm's joints attain specific distances, presumably measured during a full range of motion or a set of tasks. The data congregates around a central value, indicating a mean distance that the arm's joints most commonly reach. The spread of the data, captured by the width of the histogram, suggests variability in the arm's motion, with the tails of the distribution indicating the less frequently reached extremes [8]. Such a distribution is essential for analyzing the robotic arm's mechanical performance and movement precision, allowing engineers to identify any anomalies or variances that may affect operational efficiency or the quality of tasks performed, such as welding or part manipulation.

Table 1: The length of each link and its actuator mass of the robotic arm

Physical Parameters	L1	L2	L3	L4	L5
Length (cm)	20.37	31.73	18.21	6.12	8.45
Actuator Wt. (Kg)	1.01	0.98	0.18	0.09	0.07
Link Mass (Kg)	4.82	1.05	1.45	0.36	0.07

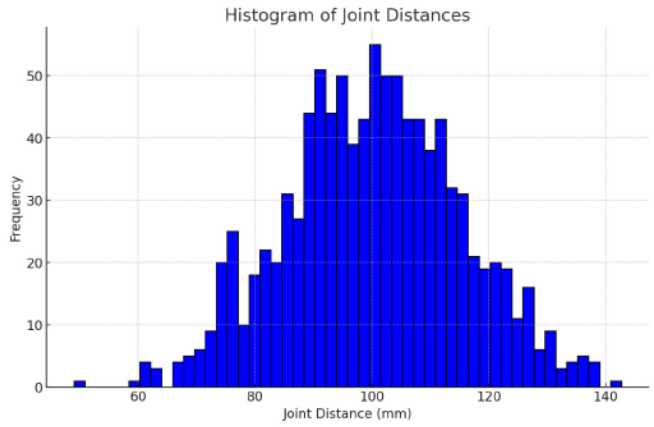

Figure 11: Histogram graph showing the distribution of joint distances for a robotic arm.

Forward and Inverse Kinematics: The forward and inverse kinematics have been suitably computed in MATLAB to reach the target coordinates from the genesis coordinates. On gauging the results, it is observed that not every position is reachable. This may not have a unique solution due to the arm's limited DOF, and certain positions may be unreachable. For real-world applications, numerical methods or optimization algorithms are often employed to find the best approximate solutions for the inverse kinematics problem [23].

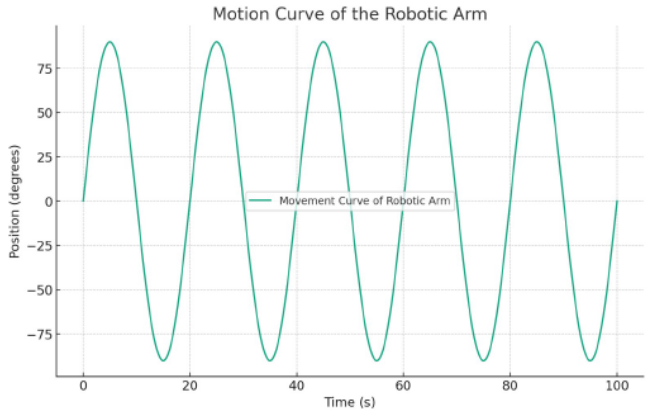

Figure 12: Motion curve of the robotic arm.

The motion curve of the robotic arm during the start-up check, depicted in Figure **12**, illustrates its harmonic movement over time. As the arm operates, it follows a sinusoidal path, indicative of the precise and repetitive tasks for which it is programmed. This pattern of motion is typical for robotic arms that perform consistent and cyclical actions [24], with the amplitude representing the extent of the arm's reach and the frequency indicating the speed of its operation. The smoothness of the curve reflects the arm's sophisticated control system, capable of executing complex tasks with high repeatability and accuracy, which is crucial in industrial automation settings.

4.3. Simulation of the Robotic Arm

Utilizing Autodesk Fusion 360, the model has been meticulously constructed to ensure that each joint, link, and end-effector's geometry matches their real-world counterparts. Fidelity is one of the major features kept in mind. The CAD model served as the blueprint for the simulation, encoding the structural and mechanical properties inherent to the robotic arm. This setup can be viewed in Figure **13**.

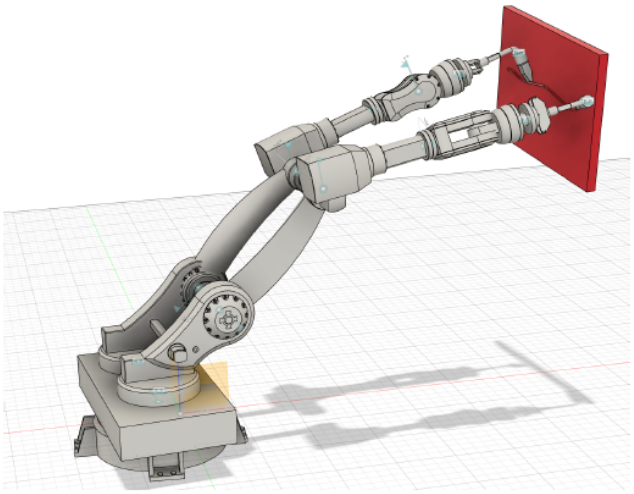

Figure 13: Simulating the robotic arm to weld the metal sheet.

With the supportive assistance from Autodesk Inventor, the model was deliberately converted into a Matlab Simscape/Simmechanics Multibody link, upon which it was imported for XML conversion. This XML file is run and a Simulink body has been generated, to which forward and inverse functions are constructed and connected to the model, as can be seen in Figure **14**.

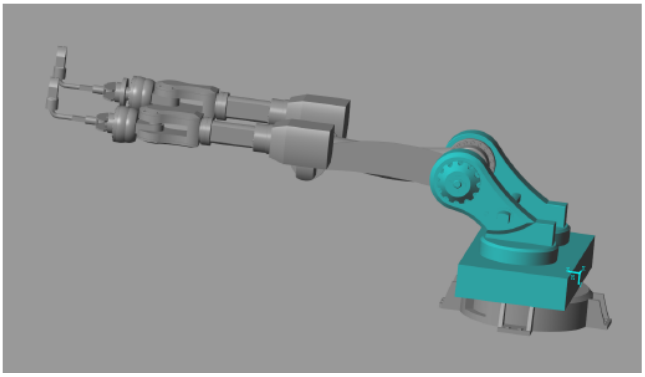

Figure 14: Matlab assembly using Simulink.

A total of 82 runs have been conducted of which the average co-ordinates have been reported. These coordinates run in the world plane (3-dimensional plane). The trajectory followed by the constructed assembly was noted down and plotted for comparison with the desired trajectory. This trajectory path is depicted in Figure **15**.

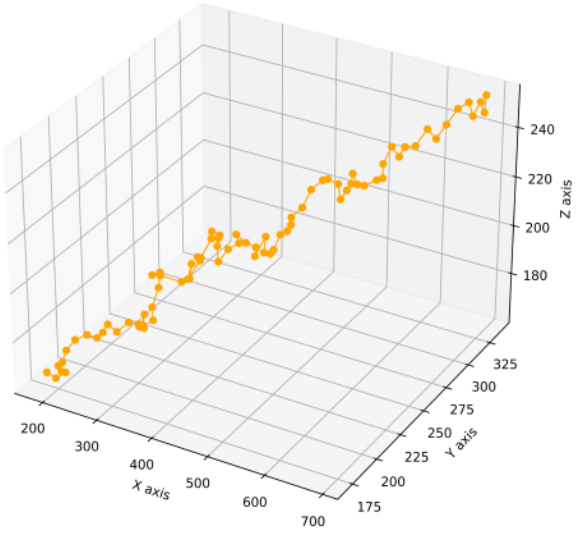

Figure 15: Trajectory path of the robotic arm.

The desired trajectory path has been designed after verifying the coordinates in an arbitrary world generated by Simscape/Inventor. Therefore, it is utilized to compare and contrast to find out the performance of the model. The coordination of the twin arms is one of the core features and most crucial parts. The cross-coordination results have come out satisfactorily with an average time of 7.1 seconds for 50.5cm shear/crack. This is verified in Figure **16** which depicts a time-series description of the operational sequence timestamps recorded in the simulation.

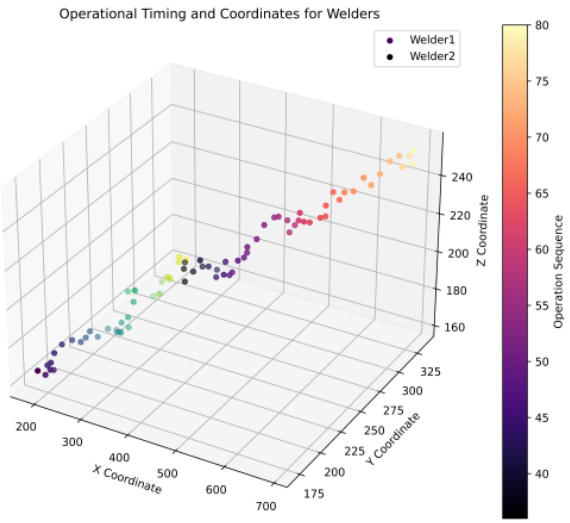

Figure 16: Time-series plot of cross-coordination.

The simulation results were twofold: Firstly, the kinematic model validated the theoretical joint movements and end-effector paths, confirming that the physical prototype should perform as expected. Secondly, dynamic simulations revealed critical insights into the system's response under various operational conditions. These results informed iterative improvements, ensuring that the robotic arm's design was functional and optimized for its intended applications.

Thus, the simulation workflow proved to be a powerful tool for promptly identifying and mitigating design and functional risks, thus significantly streamlining the development process of the robotic arm.

5. CONCLUSION

The research initiative underscores the successful development of a specialized robotic arm system for GMAW/MIG welding applications in automobile maintenance. The integration of ultrasonic sensing, a dual-arm structure for enhanced maneuverability, and the incorporation of a PID controller with a Reinforcement Learning (RL) agent marks a significant advancement in industrial automation. The RL agent, trained through extensive simulations to refine the system's accuracy and efficiency, demonstrates the system's capability to perform complex welding tasks with minimal human intervention. The result is a solution that elevates the precision and quality of welding operations and significantly contributes to the advancement of automated post-manufacturing services, promoting an economic boost by enhancing serviceability and repair quality. Furthermore, the project's success in employing Deep Cross Network (DCN) for crack detection highlights the system's adeptness in handling nuanced assessments required in damage evaluation. The project, therefore, stands as a testament to the synergy between mechanical design, electronic precision, and intelligent software processing in creating highly efficient, autonomous systems.

LIST OF ABBREVIATIONS

MAKER	MIG Assisted Kernel Enabled Robot
CAGR	Compound Annual Growth Rate
OBD	On Board Diagnostic

GMAW	Gas Metal Arc Welding
MIG	Metal Inert Gas
IoT	Internet of Things
IR 4.0	Industry Revolution 4.0
RCNN	Region-based Convolutional Neural Network
DCN	Deep Cross Network
RL	Reinforcement Learning
PID	Proportional - Integral - Derivative

ACKNOWLEDGEMENTS

This work was supported, in part, by the National Science and Technology Council, Taiwan, grant number NSTC 112-2221-E-197-015.

REFERENCES

[1] S. M. Abhay S., "Automotive repair and service market size, share, statistics. allied market researchs," Retrieved from https://www.alliedmarketresearch.com/automotive-repair-and-servicemarket, no. 2, 2022.

[2] F. Xu, Y. Xu, H. Zhang, and S. Chen, "Application of sensing technology in intelligent robotic arc welding: A review," Journal of Manufacturing Processes, vol. 79, pp. 854-880, 2022. https://doi.org/10.1016/j.jmapro.2022.05.029

[3] K. D. Thoben, S. Wiesner, and T. Wuest, "industrie 4.0" and smart manufacturing - a review of research issues and application examples," International Journal of Automation Technology, vol. 11, pp. 4-19, 01, 2017. https://doi.org/10.20965/ijat.2017.p0004

[4] B. Almannai, R. Greenough, and J. Kay, "A decision support tool based on qfd and fmea for the selection of manufacturing automation technologies," Robotics and Computer-Integrated Manufacturing, vol. 24, no. 4, pp. 501-507, 2008. ICMR2005: Third International Conference on Manufacturing Research. https://doi.org/10.1016/j.rcim.2007.07.002

[5] C. Cronin, A. Conway, and J. Walsh, "State-of-the-art review of autonomous intelligent vehicles (aiv) technologies for the automotive and manufacturing industry," in 2019 30th Irish Signals and Systems Conference (ISSC), pp. 1-6, 2019. https://doi.org/10.1109/ISSC.2019.8904920

[6] F. B. Insights, "Welding market size, share - global research report," from https://www.fortunebusinessinsights.com/industry-reports/weldingmarket- 101657, 2023.

[7] P. Kah, M. Shrestha, E. Hiltunen, and J. Martikainen, "Robotic arc welding sensors and programming in industrial applications," International Journal of Mechanical and Materials Engineering, vol. 10, p. 13, Jul 2015. https://doi.org/10.1186/s40712-015-0042-y

[8] D. Lau, "A fully automated construction industry? still a long road ahead," Retrieved from https://www.archdaily.com/945761/a-fullyautomated-construction-industry-still-a-long-road-ahead, 2020.

[9] J. A. Zamora-Nunez, R. Rodrıguez-Rosales, P. M. Trejo-Garcıa, B. R. Rodrıguez-Vargas, and A. Tahaei, "Microstructure evaluation of 304 stainless-steel welds through robotic gmaw process," MRS Advances, Nov. 2023. https://doi.org/10.1557/s43580-023-00679-y

[10] D. Curiel, F. Veiga, A. Suarez, and P. Villanueva, "Advances in robotic welding for metallic materials: Application of inspection, modeling, monitoring and automation techniques," Metals, vol. 13, no. 4, 2023. https://doi.org/10.3390/met13040711

[11] Y. Cheng, R. Yu, Q. Zhou, H. Chen, W. Yuan, and Y. Zhang, "Realtime sensing of gas metal arc welding process - a literature review and analysis," Journal of Manufacturing Processes, vol. 70, pp. 452-469, 2021. https://doi.org/10.1016/j.jmapro.2021.08.058

[12] P. Devendran and P. A. Varthanan, "Prediction of weldment mechanical properties in gmaw with robot-assisted using fuzzy logic systems," Materials Research Express, vol. 8, p. 126524, dec 2021. https://doi.org/10.1088/2053-1591/ac432a

[13] S. Ma, T. Tang, H. You, Y. Zhao, X. Ma, and J. Wang, "An robotic arm system for automatic welding of bars based on image denoising," in 2021 3rd International Conference on Robotics and Computer Vision (ICRCV), pp. 40-44, 2021. https://doi.org/10.1109/ICRCV52986.2021.9546976

[14] X. Wang, W. Li, and Z. Wu, "Cardd: A new dataset for vision-based car damage detection.," Retrieved from https://ar5iv.labs.arxiv.org/html/2211.00945, 2022.

[15] Evs Tech Co., Ltd., "Different degrees of freedom in robotics arms: A full explanation," Retrieved from https://www.evsint.com/degrees-of-freedomin-robotic-arms., 2022.

[16] NSCA's Essentials of Personal Training, Second Edition, "Kinematic and kinetic chains," Retrieved from https://www.nsca.com/education/articles/kinetic-select/kinematic-andkinetic- chains, 2017.

[17] R. Singh, V. Kukshal, and V. S. Yadav, "A review on forward and inverse kinematics of classical serial manipulators," in Advances in Engineering Design (P. K. Rakesh, A. K. Sharma, and I. Singh, eds.), (Singapore), pp. 417-428, Springer Singapore, 2021. https://doi.org/10.1007/978-981-33-4018-3_39

[18] M. Dobi˘s, M. Dekan, P. Be˘no, F. Ducho˘n, and A. Babinec, "Evaluation criteria for trajectories of robotic arms," Robotics, vol. 11, no. 1, 2022. https://doi.org/10.3390/robotics11010029

[19] S. Zhu, "Robotic GMAW forming remanufacturing technology," Advances in Manufacturing, vol. 1, pp. 87-90, Mar. 2013. https://doi.org/10.1007/s40436-013-0001-x

[20] T. M. Lubecki and F. Bai, "Weld quality assessment based on arc sensing for robotic welding," in 2015 IEEE International Conference on Advanced Intelligent Mechatronics (AIM), pp. 1496-1501, 2015. https://doi.org/10.1109/AIM.2015.7222753

[21] A. J. P. A. ChÅLavez and J. H. A. AlcÅLantara, "Kinematic and dynamic modeling of the phantomx ax metal hexapod mark iii robot using quaternions," in 2021 International Conference on Control, Automation and Information Sciences (ICCAIS), pp. 595-601, 2021.

[22] Y. Zhou, Y. Chen, C. Sun, and Q. Zhang, "Design and simulation analysis of robot-assisted plate internal fixation device for lower limb fractures," International Journal of Robotics and Automation Technology, vol. 10, p. 1-13, Jan. 2023. https://doi.org/10.31875/2409-9694.2023.10.01

[23] D. Parhi, B. Deepak, D. Nayak, and A. Amrit, "Forward and inverse kinematic models for an articulated robotic manipulator," vol. 4, pp. 2012-103, 01 2013.

[24] H. Chen, S. Ye, X. Li, and Y. Leng, "Motion planning and calculation method of power inspection robot arm," in 2023 6th International Conference on Energy, Electrical and Power Engineering (CEEPE), pp. 678-682, 2023. https://doi.org/10.1109/CEEPE58418.2023.10167068

[25] J. Yang, G. Zhang, L. Wang, J. Wang, and H. Wang, "Multi-degree-of-freedom joint nonlinear motion control with considering the friction effect," IEEE 19th World Symposium on Applied Machine Intelligence and Informatics (SAMI), Herl'any, Slovakia, pp. 211-216, 2021. https://dx.doi.org/10.1109/SAMI50585.2021.9378674

[26] X. Wang, Q. Chen, H. Sun, X. Wang, and H. Yan, "GMAW welding procedure expert system based on machine learning, " Intelligence & Robotics, vol. 3, no. 1, pp. 56-75, 2023. https://dx.doi.org/10.20517/ir.2023.03

[27] S. A. Kumar, R. Chand, R. P. Chand, and B. Sharma, "Linear manipulator: Motion control of an n-link robotic arm mounted on a mobile slider," Heliyon, vol. 9, no. 1, pp. e12867, 2023.

Received on 02-11-2023 Accepted on 24-11-2023 Published on 15-12-2023

DOI: https://doi.org/10.31875/2409-9694.2023.10.10